Titre: Title:	Long-term fluorescence hyperspectral imaging of on-chip treated co-culture tumour spheroids to follow clonal evolution
Auteurs: Authors:	Amélie St-Georges-Robillard, Maxime Cahuzac, Benjamin Péant, Hubert Fleury, Muhammad Abdul Lateef, Alexis Ricard, Alexandre Sauriol, Frédéric Leblond, Anne-Marie Mes-Masson, & Thomas Gervais
Date:	2019
Type:	Article de revue / Article
Référence: Citation:	St-Georges-Robillard, A., Cahuzac, M., Péant, B., Fleury, H., Lateef, M. A., Ricard, A., Sauriol, A., Leblond, F., Mes-Masson, A.-M., & Gervais, T. (2019). Long-term fluorescence hyperspectral imaging of on-chip treated co-culture tumour spheroids to follow clonal evolution. Integrative Biology, 11(4), 130-141. https://doi.org/10.1093/intbio/zyz012

Titre de la revue: Journal Title:	Integrative Biology (vol. 11, no. 4)
Maison d'édition: Publisher:	Oxford Academic
URL officiel: Official URL:	https://doi.org/10.1093/intbio/zyz012
Mention légale: Legal notice:	This is a pre-copyedited, author-produced version of an article accepted for publication in Integrative Biology (vol. 11, no. 4) following peer review. The version of record St-Georges-Robillard, A., Cahuzac, M., Péant, B., Fleury, H., Lateef, M. A., Ricard, A., Sauriol, A., Leblond, F., Mes-Masson, A.-M., & Gervais, T. (2019). Long-term fluorescence hyperspectral imaging of on-chip treated co-culture tumour spheroids to follow clonal evolution. Integrative Biology, 11(4), 130-141. https://doi.org/10.1093/intbio/zyz012 is available online at: https://doi.org/10.1093/intbio/zyz012.

Long term fluorescence hyperspectral imaging of on-chip treated co-culture tumour spheroids to follow clonal evolution

Amélie St-Georges-Robillard,[1,2] **Maxime Cahuzac,**[2] **Benjamin Péant,**[2,3] **Hubert Fleury,**[2] **Muhammad Abdul Lateef,**[2] **Alexis Ricard,**[2] **Alexandre Sauriol,**[2] **Frédéric Leblond,**[1,2] **Anne-Marie Mes-Masson,**[2,4] **Thomas Gervais**[1,2,*]

[1] Polytechnique Montréal, Department of Engineering Physics and Institute of Biomedical Engineering, Montreal, H3C 3A7, Canada
[2] Centre de recherche du Centre hospitalier de l'Université de Montréal and Institut du cancer de Montréal, Montreal, H2X 0A9, Canada
[3] TransMedTech Institute, Montréal, H3T 1J4, Canada.
[4] Université de Montréal, Department of Medicine, Montreal, H3T 1J4, Canada
* thomas.gervais@polymtl.ca

Received: 17th December 2018
Accepted: 30th May 2019
First published: 7th June 2019

Integrative Biology, Volume 11, Issue 4, April 2019, Pages 130–141
DOI: 10.1093/intbio/zyz012

ABSTRACT

Multicellular tumour spheroids are an ideal *in vitro* tumour model to study clonal heterogeneity and drug resistance in cancer research because different cell types can be mixed at will. However, measuring the individual response of each cell population over time is challenging: current methods are either destructive, such as flow cytometry, or cannot image throughout a spheroid, such as confocal microscopy. Our group previously developed a wide-field fluorescence hyperspectral imaging system to study spheroids formed and cultured in microfluidic chips. In the present study, two subclones of a single parental ovarian cancer cell line transfected to express different fluorophores were produced and co-culture spheroids were formed on-chip using ratios forming highly asymmetric subpopulations. We performed a 3D proliferation assay on each cell population forming the spheroids that matched the 2D growth behaviour. Response assays to PARP inhibitors and platinum-based drugs were also performed to follow the clonal evolution of mixed populations. Our experiments show that hyperspectral imaging can detect spheroid response before observing a decrease in spheroid diameter. Hyperspectral imaging and microfluidic-based spheroid assays provide a versatile solution to study clonal heterogeneity, able to measure response in subpopulations presenting as little as 10% of the initial spheroid.

INSIGHT BOX

Microfluidic chips are known to be able to form and culture hundreds of tumour spheroids easily. However, measurement techniques routinely used, such as confocal microscopy, light sheet microscopy, or flow cytometry, are not adapted for the *in situ* analysis of this massive number of samples. This work reports how wide-field hyperspectral imaging can be used to follow the treatment response of individual fluorescent cell populations in spheroids non-destructively and in a high-throughput manner. The method described here further reveals the onset of clonal takeover in 3D co-cultures with similar drug resistance. This work represents the first step towards using

hyperspectral imaging to analyse spheroids in microfluidic chips, opening the possibilities of future chip-based spheroid research.

Introduction

Many types of cancer, including ovarian cancer, are characterised by the presence of clonal heterogeneity, where tumours are composed of multiple populations of malignant subclones with different genetic mutations. These subclones can then each evolve differently over time and in response to treatments. Treatment affecting one subclone can lead to tumour repopulation by a different and possibly more resistant subclone. Cancers with high levels of clonal heterogeneity are thus associated with poor prognosis, treatment resistance, and an increased difficulty to develop biomarkers of prognosis or treatment response [1]–[3]. To study clonal heterogeneity, monolayer co-culture of cancer cells can be used as an *in vitro* cancer model. However, there is now evidence that 3D cellular models, such as spheroids, are more relevant than 2D cell culture as *in vitro* cancer models for drug discovery [4]. Spheroids are 3D cell aggregates that better reproduce cell-cell and cell-matrix interactions [5]–[7]. They also incorporate fundamental mass transfer limitations important in most cellular response to drugs [8]. By mixing two or more cell lines in a single spheroid, researchers can improve their relevance and include clonal heterogeneity in their studies. Informative assays include mixing epithelial and stromal cells, resistant and sensitive cells, or cancer and immune cells.

The microfluidics community has provided numerous tools that can easily perform assays on 3D tissue models such as spheroids, organoids [9], and micro-dissected tissues [10]. Researchers have developed chips that can form up to thousands of spheroids in one step and expose them to external stimuli [11]–[17]. Chips are especially useful to hold or trap spheroids in place during medium changes or when adding drugs of interest without the risk of pipetting them out of plate wells [18]–[20]. However, there remains important challenges including methods that analyse sample dynamics, including tracking cell populations in co-culture spheroids.

To study these co-culture spheroids in terms of proliferation, response to treatment, or invasion, each cell population composing the spheroids must be studied independently rather than measuring whole spheroid response [21] as cell populations can compete or co-operate for survival against a drug within a spheroid [22]. These constraints greatly restrict the number of methods that can be employed to analyse this response. For example, diameter or volume measurements, often reported in the literature as a metric of spheroid response [23]–[25], can no longer be applied to determine cell population-specific responses.

Over the years, several methods have been developed to distinguish subclonal population growth within a multicellular system whether spheroids were formed in microfluidic chips or using conventional methods. Techniques are either based on cell morphology [26], colorimetric or fluorescent antigen stains [23], genetic modifications to inherently express different fluorescent markers, or viability dyes [23]. When these markers are used in 2D monolayer culture, conventional microscopes can distinguish individual cells. Cells can then be counted visually according to whether they present the markers or not. However, the same technique cannot be applied to 3D tissue analysis unless spheroids are first digested into a single cell suspension.

In response, a lot of effort has been applied to adapting fluorescence-based methods to correctly quantify cell populations in 3D cultures using either fluorescent proteins [27], fluorescent

trackers or viability dyes [28], [29]. A conventional optical fluorescence microscope can quantify spheroid fluorescence intensity if parameters during the image acquisition are known and controlled [23], [30]. However, most optical microscopes are designed to image cell monolayers using a depth of field corresponding to the size of a cell. If used to image 3D cultures, a slightly out of focus sample can drastically affect the measured fluorescence intensity [31], [32]. This hinders precisely quantifying spheroid fluorescence using conventional optical microscopes and limits their usefulness. Confocal microscopy was developed to image virtual optical sections of 3D samples individually using pinholes to reject light from out of focus planes of the sample. Fluorescent cells can then be counted on each slice. However, this optical sectioning is done at the cost of lower signal intensity and, coupled with tissue absorption and scattering, limits light penetration in the centre of a biological sample. Samples thicker than 70-100 μm are thus more difficult to image [23], [33], [34], or need to be optically cleared [35], [36]. Multiphoton microscopy can circumvent this by taking advantage of the near-infrared optical window, a range of wavelengths between 650 and 1 300 nm where light penetration depth is the highest in tissues. However, to achieve multiphoton excitation of fluorophores, objectives with high numerical apertures and shorter working distances are needed, rendering imaging thick (> 5 mm) microfluidic chips difficult [37]. For all three types of microscopy, the typical filter cubes used reduce their spectral resolution and increases cross-talk between fluorescence channels, limiting which and how many fluorophores can be imaged, especially when large spectral overlaps exist [30]. Flow cytometry or fluorescence activated cell sorting (FACS) can resolve a large number of fluorescent markers but require spheroid digestion into individual cells before analysis [38]. Studying the same sample over time is impossible using this type of destructive technique. Finally, immunohistochemistry and immunofluorescence performed on tissue slices (paraffin embedded or cryosections) are also used but present the same drawback as FACS as they are destructive techniques [23].

In this paper, we describe a method using hyperspectral imaging (HSI) to quantify cell populations over time in co-culture spheroids in response to external stimuli. The HSI system was optimised to analyse multiple spheroids on-chip in a single acquisition. Co-culture spheroids expressing two fluorescent proteins were formed directly on-chip and their growth was followed over time as a function of the initial cell seeding ratio. Based on the different proliferation rates for each fluorescent subclone, we hypothesised that hyperspectral imaging could also be used to study the dynamic effect of chemotherapy drugs affecting DNA such as PARP inhibitors [39] and platinum-based drugs [40] in cell populations with distinct growth properties. We then studied spheroid response to different chemotherapy drug concentrations and measured each fluorescent population's dynamic response to the drug over time. Our method has the advantage of being non-destructive: the dynamic response of each cell population in the spheroids can be followed at multiple time-points over time and large numbers of spheroids can easily be measured. Three sets of experiments are described in this work illustrating the potential of hyperspectral imaging for spheroid-based research.

Results

Hyperspectral imaging workflow to quantify cell populations in co-culture spheroids

Fig. 1 introduces the workflow presented in this article. We first produced fluorescent subclones of the ovarian cancer cell line OV1946 [41]. This cell line, established from patient ascites, can form spheroids in a low attachment environment. In a previous study [42] we observed that subclones made from two different parental cell lines did not mix homogeneously in spheroids and remained as distinct aggregates. As cell-cell interactions are an important factor in studying cancer and drug resistance [43], we chose to use a single ovarian cancer cell line to make two fluorescent subclones with the hypothesis that the two cell populations would mix homogeneously. The two fluorescent populations were produced by transfecting OV1946 cells with enhanced Green Fluorescent Protein (eGFP) (eGFP-OV1946) and mCherry (mCherry-OV1946) plasmids. Two subclones from the transfected populations were selected by limited dilution to obtain cells expressing each fluorescent protein at similar intensity for a specific subclone, as illustrated in step 1 of Fig. 1.

The two fluorescent subclones were then mixed at different ratios to form co-culture spheroids on-chip. Various cell seeding ratios were studied: 100:0, 90:10, 75:25, 50:50, 25:75, 10:90, and 0:100 (eGFP:mCherry). The microfluidic chip used to form these spheroids is based on Patra *et al*. [14] and is composed of a main channel with groups of 24 wells placed underneath. Cells sediment in the wells and form one spheroid per well in 24 h. Their compactness depends on the cell line used. Spheroids were then cultured on-chip up to nine days after formation. Medium was changed every 24 h to replenish the nutrients available to the spheroids and remove their waste, in compliance with previously published on-chip 3D cell culture guidelines [44].

Hyperspectral imaging was used to image one group of 24 spheroids trapped on-chip in a single hyperspectral acquisition. HSI images were acquired with the system illustrated in Fig. 1 and calibrated using the image analysis steps described in detail previously [42] to extract the true fluorescence intensity emitted by the sample from the system response. These steps are also detailed in the Materials and Methods section. As both fluorescent subclones emit the same fluorescence intensity for all their cells, and that intensity is not the same for both subclones, both proteins' intensities were normalised before calculating the proportion of each cell population in the spheroids. An average intensity of the fluorescence in regions of interest corresponding to each spheroid at day 0 was used as a reference.

2D proliferation assay on cell populations

While creating the eGFP and mCherry subclones by transfection, we selected clones with different proliferation rates to see if HSI is able to measure this difference while forming co-culture spheroids. Fig. 2 shows the standard 2D proliferation assay performed to measure the proliferation rate of each subclone. Fig. 2A-C shows the proliferation of each subclone cultured independently, where eGFP-OV1946 cells doubling time is 1.5 times faster than mCherry-OV1946. When eGFP cells were mixed at different ratio with mCherry cells, they again proliferated faster than mCherry cells (Fig. 2D-F).

FACS validation

Before using hyperspectral imaging to quantify spheroid composition, we first validated that spheroid composition measurements obtained by HSI were similar to those obtained by FACS. Spheroids were made on-chip according to the same initial seeding ratios described previously. They were then cultured on-chip for 3 to 6 days, depending on the experiment (n = 3). Medium was changed daily. For this validation, 3 groups of 24 wells per chip were first imaged individually using HSI and the same spheroids were then pooled and analysed by FACS (Fig. 3A). Fig. 3B shows that HSI has an absolute error in spheroid composition percentage of at most 5% when compared to FACS.

3D proliferation assay on cell populations

Using our HSI system and its image analysis algorithm, we validated that similar trends in the proliferation of both subclones in 2D could be observed in a 3D spheroid. The 3D proliferation assay timeline on cell populations is detailed in Fig. 4A. Spheroids were formed on-chip at various initial seeding ratios (100:0, 90:10, 75:25, 50:50, 25:75, 10:90, and 0:100) and 24 spheroids per ratio were imaged daily until day 9. The experiment was repeated three times. Step 7 of Fig. 1 presents representative fluorescence and brightfield images of a co-culture spheroid made with subclone of the same parental cell line, confirming our hypothesis that the two subclones would mix homogeneously. Fig. 4B shows the brightfield images of one representative spheroid per ratio over time. We observed that compact spheroids were formed on day 2 and individual spheroid diameter then increases over time as cells proliferate. However, brightfield images alone cannot distinguish the individual growth rate of eGFP or mCherry cells. We tested the ability of fluorescence measurements by HSI to track cell population growth over time. Fig. 4C i and iii show the spheroid composition in eGFP and mCherry cells for each initial seeding ratio. The same curves normalised to day 1 are shown in Fig. 4C ii, iv, and v. We noted that eGFP cells first experience a rapid proliferation from day 0 up to day 5, doubling their fluorescence intensity. Their proliferation then decreased until day 9. Shaded areas represent error bars (standard error of the mean, n = 3) and illustrate how eGFP cells' behaviour varies between the experimental repetitions. Noteworthy, even if the total number of cells in each spheroid at day 0 was the same, eGFP cells in spheroids composed mainly of mCherry cells grew more than in those made only of eGFP cells (Fig. 4C ii). In contrast, as highlighted by the smaller error bars, mCherry cells proliferation remains constant from experiment to experiment. Their proliferation is slower than eGFP cells, but continues until day 9, where their fluorescence intensity was doubled compared to day 0. Also, we did not observe a dependence on the initial number of mCherry cells as mCherry cells in all spheroids grew at the same rate (Fig. 4C iv). Importantly, when comparing subclones proliferation up to day 5 (Fig. 4C v), we can see that eGFP cells grew faster than mCherry cells in earlier days, replicating the biological characteristics observed in 2D cultures.

In addition to following each cell population's fluorescence intensity over time, we also calculated the proportion occupied by each population in the spheroids. eGFP and mCherry fluorescence intensities were first normalised to a reference intensity so that both intensities could be compared, and the spheroid composition was calculated with equation 1 (see Materials and Methods). Fig. 4D utilises a stacked area chart to represent the spheroid composition over time as a function of the initial seeding ratio. The proportion occupied by eGFP cells is represented by the bottom (green) area while the top (red) area represents the proportion occupied by mCherry cells. In the first 5 days, we can see a slight increase of the percentage of eGFP cells, correlating to their

higher proliferation rate of the first days. At day 9, the spheroid composition then returns around the initial composition of day 0. This contrasts with results from 2D culture, where eGFP cells continued to proportionally occupy more space than mCherry cells (Fig. 2D-F). This could be explained by effects unique to spheroids, such as competition for space within the 3D volume.

Treatment response assay on cell populations

Clonogenic assays were performed to assess each subclone's response to the PARP inhibitor talazoparib. Fig. S1 shows that the eGFP subclone is slightly more resistant than the mCherry subclone, although this difference is not statistically significant: eGFP cells have a 2D concentration at which 50% of colony formation is inhibited (IC_{50}) of 27.7 ± 2.0 nM and mCherry cells, of 21.2 ± 6.0 nM. Knowing that 2D and 3D culture can have different responses to treatment [8], [45], we hypothesised that HSI could follow each cell population response independently and observe differences in response. A treatment response assay was performed by exposing the same co-culture spheroids, made at the same seeding ratio as previously, to three concentrations of drug from day 2 to day 9 (Fig. 5A). The experiment was repeated three times. Fig. 5B shows brightfield images of representative spheroids at day 8, depending on the treatment concentration, while Fig. 5C shows brightfield images of spheroids over time as they are exposed to the highest talazoparib concentration (50 μM). For a specific seeding ratio, the evolution of the same spheroid over time is shown. The fluorescence intensity of each cell population measured by HSI is shown in Fig. 5D-E. Each graph presents the response of 24 spheroids made at a specific seeding ratio to the three talazoparib concentrations and the talazoparib vehicle (medium and DSMO). In each graph, we observed a dose-response effect, where fluorescence intensity (both eGFP and mCherry) decreases after exposure to the drug starting at day 2. For both cell lines, 5 nM is too low to elicit a response, as the curves are similar to those of the control with no drug. However, for the highest concentration, we can clearly see fluorescence decreases sharply for both cell populations, indicating that cells are affected by the treatment between day 3 and 4 (after 24-48 h of treatment), which is consistent with the subclones doubling time. Using the HSI, the treatment effect was detected earlier, as spheroid diameters at day 8 (Fig. 5B) are just starting to diminish at the highest concentration. While curves for spheroid with low starting number of cells are noisier due to a lower signal intensity (Fig. 5D i and 5E vi, for example), they still demonstrate that our method can measure treatment response of cell populations occupying as little as 10% of the spheroid.

Fig. 6 presents the spheroid composition as a response to the three talazoparib concentrations. At 5 nM (Fig. 6A), both cell populations react similarly to the control (Fig. 4D). At the intermediate concentration of 500 nM (Fig. 6B), the eGFP percentage seems to increase very slightly over time. At the highest concentration of 50 μM, we can observe that the spheroids experience a clonal takeover by mCherry cells. Both cell populations die from talazoparib, as illustrated by Fig. 5D-E, but mCherry-OV1946 cells seem more resistant and die less, proportionally. Independent of the initial cell seeding ratio, this takeover starts consistently at day 4, after 48h of treatment. While Fig. 5D-E present how each subclone responds to treatment, Fig. 6 reveals the behaviour differences between the two subclones.

As a proof of concept that HSI can also measure treatment response of spheroids exposed to platinum-based drugs, we formed co-culture spheroids using the following seeding ratios: 100:0, 50:50, and 0:100, and exposed them to carboplatin from day 1 to day 3 (Fig. 7A). The experiment was performed once (n = 1) on 24 spheroids per condition (ratio and drug concentration). Fig. 7B

shows that, similar to the treatment response assay to talazoparib, spheroid diameters as a metric to measure treatment response is not always appropriate. Fluorescence intensities over time (Fig. 7C) show a dose-dependent decrease in day 1 fluorescence intensities for both subclones. At the two highest carboplatin concentrations (300 μM and 3 mM), both subclones start to die between day 1 and day 3. At the low concentration of 30 μM, the fluorescence intensities do not immediately decrease from day 1 to day 3, but instead, the decrease starts after the chemotherapy is removed: mCherry intensity starts to decrease 24 h after eGFP intensity. This difference can also be observed on the corresponding spheroid composition graph and is highlighted by arrows. From day 0 to day 3, the spheroid composition in eGFP-OV1946 cells increases consistently. Between day 3 and day 4, eGFP-OV1946 cells are more affected by the treatment than mCherry-OV1946 cells, resulting in a steep decrease in eGFP spheroid composition. From day 4 to the end of the experiment, mCherry-OV1946 cell death reaches similar rates as eGFP-OV1946 cells and the spheroid composition stabilises.

Discussion and Conclusion

Many research groups have developed methods using various combinations techniques to study co-culture spheroids and follow their cell populations over time. Several of these methods are either based on destructive techniques such as digesting spheroids prior to analysis [21], [28], [29], cryosections [27], [28], or flow cytometry [28], [29], or on confocal microscopy [27]. These methods cannot achieve long term repeated analyses of the same spheroids over time while also sampling the centre of larger spheroids (> 70-100 μm). Our method, based on forming and treating spheroids on-chip, and following their fluorescence over time using wide-field hyperspectral imaging, has the advantages of being rapid, precise, and versatile. Multiple samples can be imaged in the wide field of view. We were able to measure 24 spheroids for 28 conditions each (7 ratios x 4 drug concentrations) in a single experimental run, taking approximately 4 hours to perform. If confocal or multiphoton imaging were to be done in 30 seconds for each spheroid, as it is customary, 5.6 hours would have been required just to perform the imaging step. The hyperspectral capabilities of the system can distinguish fluorophores with close emission peaks or fluorophores of low intensity overshadowed by a fluorophore of higher intensity, as demonstrated in our previous work [42]. Finally, since the excitation wavelength of the HSI system can be chosen between 400 and 700 nm and the emitted fluorescence can be measured from 450 to 720 nm, the system is highly versatile in terms of which fluorophores can be imaged. Overall, our microfluidic chip and our hyperspectral imaging system can generate and treat spheroids rapidly with an absolute error of less than 5% in spheroid composition compared to FACS analysis.

The 2D proliferation assay showed that one subclone, eGFP-OV1946, has a doubling time 1.5-times faster than the mCherry subclone when cultured separately. Cultured together at different seeding ratios, eGFP-OV1946 also proliferated faster than mCherry-OV1946 cells. This trend was also observed in spheroids using the HSI system, although eGFP-OV1946 cell proliferation decreased starting at day 5 of spheroid culture. Our method to assess treatment response on ovarian cancer spheroids also illustrates how, depending on the cell line and drug studied, using fluorescence can detect treatment response earlier than the spheroid diameter.

We observed that a concentration as high as 50 μM was necessary to illicit a clear decrease in fluorescence, especially for eGFP cells, even if the 2D IC50 of both subclones is between 20 and 30 nM. At the 500 nM drug concentration (around 20X of the 2D IC_{50} for both cell lines), a slight

decrease in fluorescence compared to the control and the 5 nM concentration was observed (Fig. 5D-E). This result is typical of treatment response in 3D cultures, as the drug concentrations necessary to elicit a drug response are normally higher in 3D than in 2D [46]. Other experimental work in our laboratory also indicate that drug concentrations around 100X the 2D IC_{50} are necessary to elicit a response in ovarian cancer spheroids [8], [45].

One advantage of using HSI to follow cell populations over time is that we were able to measure treatment response of a cell population representing only 10% of the spheroid composition (Fig. 5D i and 5E iv). Typical studies on clonal population either can detect subclones of 10% but are destructive, or cannot follow over time such a low population [21], [29]. Our HSI system offers advantages in terms of imaging highly asymmetrical populations compared to conventional fluorescence microscopy where crosstalk can cause inaccuracy when measuring each population fluorescence intensity [30]. Finally, using the carboplatin treatment response results, we showed how breaks in the spheroid composition curve over time (Fig. 7D ii-iii) can highlight changes in the cell populations response to treatment and indicate periods of interest to study treatment response.

In conclusion, this work introduces a novel method to rapidly and dynamically analyse the response to external stimuli of highly asymmetrical co-culture spheroids formed in microfluidic chips. As HSI has demonstrated it can image and quantify three or more fluorophores without increasing experimental time [42], mixing more than two types of cells, such as epithelial and stromal cells, resistant and sensitive cells, or cancer and immune cells could be done. Our work could be applied to other types of assays, such as drug penetration in tissue studies, invasion assay, or angiogenesis studies and could find applications in high throughput/high content drug screens on spheroids to test new or known drugs on co-culture spheroids. HSI is also compatible with recently emerging *ex vivo* tumour on a chip models [47].

Materials and methods

Microfluidic chip

Spheroids were formed directly inside a microfluidic chip using a design and technique described previously [42]. The chip consists of a main channel of 2.5 mm in width and 500 μm in height with wells of 500 x 500 x 500 μm^3 placed underneath. 120 wells are placed in 5 groups of 24 to form spheroids using a single cell suspension. Spheroids stay trapped in the wells when the medium (containing drugs or not) in the main channel is changed using a low flow rate [44]. Photographs of the chip are presented in Fig 1.

Two poly(methyl methacrylate) (PMMA) moulds were micromachined using a computerised numerical control (CNC) machine (EMCO PC Mill 55, EMCO GmbH, Austria); one for the layer containing the main channel and inlets/outlets, and one for the layer containing the wells. Degassed poly(dimethylsiloxane) (PDMS, Sylgard® 184 silicone elastomer kit, Dow Corning, USA) mixed at a 10:1 ratio was then poured onto each PMMA mould and cured in an oven at 80 °C for 1 h. Both PDMS layers were exposed 30 s to an atmospheric plasma (Dyn-A-Mite, Enercon, USA) and bonded together to form the microfluidic chip. Hollow nylon cylinders (91145A138, McMaster-Carr, USA) were then introduced in the inlets and outlets.

Microfluidic chips were prepared for cell culture by first removing any bubbles in the channels using 100% ethanol followed by a 70% ethanol incubation for 10 minutes to sterilise the chip.

Channel walls were then passivated to prevent cell adhesion to the PDMS by introducing a solution of triblock copolymer block (10 mg/mL, Pluronic® F-108, 542342, Sigma-Aldrich, USA) in the channels. Chips were put in a sterile humidity chamber (plastic box with a tissue moistened with sterile water) to prevent evaporation and incubated with the passivating solution for at least 1 h or overnight at 37 °C and 5% CO_2. A final sterilisation step of ethanol 70% for 10 minutes was followed by a rinsing of the channel with sterile Hank's Balanced Salt Solution (HBSS, 311-516-CL, Wisent Inc., Canada) supplemented with 600 µg/L amphotericin B (450-105-QL, Wisent Inc.) and 55 mg/L gentamicin (450-135-XL, Wisent Inc.). Chips could then be stored at 4 °C or used immediately to form spheroids on-chip.

Co-culture spheroids

The ovarian cancer cell line OV1946 was previously established from patient ascites [41]. OV1946 cells possess the ability to form spheroids in low attachment conditions. Two fluorescent subclones were produced by transiently transfecting OV1946 cells with an eGFP plasmid (pEGFP-N1, 6085-1, Clontech Laboratories Inc., USA) and a mCherry plasmid (mCherry2-N1, #54517, Addgene, USA). Plasmid mCherry2-N1 was a gift from Michael Davidson. Successfully transfected cells were selected using G418 (500 µg/mL, Geneticin®, 10131-035, Thermo Fisher Scientific, USA). Single clones from each transfection were finally produced by limited dilution to obtain two OV1946 subclones expressing each fluorophore at the same level for all cells within a subclone.

Co-culture spheroids were formed on-chip by first mixing eGFP-OV1946 and mCherry-OV1946 cells at the following initial seeding ratios: 100:0, 90:10, 75:25, 50:50, 25:75, 10:90, and 0:100 (eGFP:mCherry). The total number of cells for all cell suspensions was 9 x 10^5 cells per millilitre of OSE medium without phenol red (316-031-CL, Wisent Inc.) supplemented with 10% foetal bovine serum (FBS, 080-150, Wisent Inc.), 55 mg/L gentamicin, 600 µg/L amphotericin B, and 500 µg/mL G418. Complete OSE medium supplemented with G418 is referenced throughout this work as “medium”, except where specified.

Spheroids were formed on-chip on day 0 by introducing 100 µL of cell suspension in the plastic cylinder of the inlet and quickly removing 100 µL of liquid from the outlet. This step was repeated 6 times to ensure a uniform distribution of cells in the chip. 24 h later, one spheroid per well was visibly formed. Experiments were started on day 2. To remove cell wastes and replenish nutrients, medium was changed every 24 h by adding 70 µL of new medium in the inlet and removing 3 x 20 µL from the outlet, 3 times to prevent ejecting spheroids from their well. Throughout the experiment, chips were incubated at 37 °C and 5% CO_2 while placed in a humidity chamber to prevent medium evaporation.

To perform a drug response assay using PARP inhibitors, talazoparib (HY-16106, MedChemExpress, USA) was first solubilised in dimethyl sulfoxide (DMSO) (D8418, Sigma-Aldrich) at 20 mM. This solution was then diluted to 5 nM, 500 nM, and 50 µM in medium. DMSO was added to each solution, including the control, to match the final DMSO concentration of 0.25% (v/v) in the 50 µM solution. To perform a drug response assay using a chemotherapy drug, carboplatin (10 mg/mL, Omega Laboratories Limited, Canada) was diluted to 30, 300, and 3 000 µM in medium.

Hyperspectral imaging system

A custom-built hyperspectral imaging system was previously developed [42] to acquire fluorescence hyperspectral data cubes (pixel x pixel x nm) of multiple spheroids trapped in a microfluidic chip with a 22.6 line-pairs per millimetre spatial resolution and a 7 nm spectral resolution. The HSI system has a field of view of 7.25 mm in diameter and can image 24 wells/spheroids of the microfluidic chip described earlier. Briefly, the HSI system is composed of two illumination branches: a halogen white light (HL-2000, Ocean Optics, USA) is used for brightfield illumination and a supercontinuum laser (Fianium, NKT Photonics, Denmark) coupled to a laser line tuneable filter (LLTF, Photon etc, Canada) is used for fluorescence excitation at various wavelengths. The illuminations are combined using a 50:50 beamsplitter (BS013, Thorlabs, USA) towards the sample. A fixed focal length objective (59-871, Edmund Optics, USA), a longpass filter (FELH0500 or FELH0550, Thorlabs), a relay lens (67-422, Edmund Optics) and a liquid crystal tuneable filter (LCTF, VariSpec VIS, Perkin-Elmer, USA) form the sample image on an electron multiplying charged-coupled device (EMCCD) camera (HNü 512, Nüvü Caméras, Canada). A custom LabVIEW 2014 (National Instruments, USA) software sweeps the tuneable liquid crystal filter to acquire images at every 5 nm and measure the sample's fluorescence emission spectrum or transmittance.

In this work, excitation wavelengths used were 480 nm for eGFP and 530 nm for mCherry. The fluorescence emission spectra were acquired from 400 to 720 nm or 550 to 720 nm, depending on the excitation wavelength used. Typical acquisition time for an image at one wavelength was 500 to 1000 ms and gain was set at 500. For each microfluidic chip, the middle group of wells was imaged, resulting in 24 spheroids imaged per condition. For the comparison with flow cytometry, 3 groups of 24 spheroids were imaged per chip (72 spheroids in total).

Brightfield and fluorescence hyperspectral data cubes of each chip imaged were analysed with a series of steps described in detail in our previous study [42]. Briefly, each data cube was first divided by its acquisition time and gain. Dark noise acquired when closing the camera shutter was then subtracted. A shading correction was then applied to compensate for uneven illumination and detection.

Fluorescence image analysis

Hyperspectral data cubes were processed using MATLAB R2015a (The MathWorks, Inc., USA) to extract the fluorescence intensity emitted by each spheroid. Since the exact positioning of the chip in the field of view of the HSI system is different for each day and chip, regions of interest (ROI) corresponding to each well of the chip were determined by registering each image with a reference image, where well positions are known. Spectral unmixing is then performed on each selected ROI to separate each spectral entity contribution using a library of previously acquired fluorescence spectrum of the fluorophores of interest. The coefficients obtained for eGFP and mCherry were used as the fluorescence intensity emitted by each fluorescent protein. This is more precise than using the fluorescence intensity at the emission peak, especially in the case of overlapping fluorophores spectra.

Because of the limited dilution performed to select one clone after transfection, all the eGFP-OV1946 (or mCherry-OV1946) cells express the eGFP (or mCherry) protein at a very similar level. However, that intensity level is not the same for both fluorescent subclones. To be able to compare eGFP and mCherry intensities, both intensities need to be normalised. Fluorescence

intensities at day 0 were averaged for all spheroids that had the same initial seeding ratio (all spheroids made at 25:75 were averaged at day 0 and fluorescence values were reported for eGFP 25% and mCherry 75%, regardless of the drug concentration tested after). A linear fit was performed, and the fit was then used to obtain an intensity for a spheroid made at 100% of each subclone. An example of this linear fit is presented in Fig. S2. These reference intensities were used to normalise all acquired data. Spheroid composition was then calculated as follows:

$$\%_A = \frac{I_A}{I_A + I_B} \times 100 \quad (1)$$

where $\%_A$ is the percentage of the spheroid composed of subclone A, $I_{A/B}$ is subclone A/B normalised intensity for this spheroid.

FACS validation

Co-culture spheroids at various seeding ratios were formed on-chip according to the method described above. Spheroids were cultured on-chip and medium, supplemented with 0.25% (v/v) DMSO, was changed every day. The experiment was repeated three times and depending on the experiment repetition, spheroids were cultured 3, 4, or 6 days on-chip. Three groups of 24 spheroids were imaged by HSI per chip and their composition in eGFP and mCherry cells was calculated and averaged. On the same day, the chips were cut to separate the same three groups of 24 spheroids which were imaged. These spheroids were harvested from the chip by peeling apart the two layers of PDMS and collecting them in a 1.5 ml tube with 100 µl of phosphate buffered saline (PBS, 311-012-LL, Wisent Inc.). The spheroids were digested by adding 100 µl of trypsin 0.05% (325-041, Wisent Inc.) for 30 seconds. Trypsin was then neutralised by the addition of 200 µl of FBS. The single cell suspension obtained was centrifuged at 1 200 rpm for 10 minutes at 4 ºC, washed with PBS, and the pellet was reconstituted in FACS buffer [PBS supplemented with 2% FBS, 1 mM EDTA (EDT001, Bioshop, Canada), and 0.1% sodium azide (V015-05, JT Baker, USA)]. The samples were read in a BD LSRFortessa (BD Biosciences, Canada) cell analyser. Results were analysed with FlowJo v10 (FlowJo, LLC, USA).

2D proliferation assay

A 2D proliferation assay was performed to determine fluorescent subclone proliferation rates. A total of 750 cells from both subclones were seeded in 96-well plates in OSE medium. Cells were imaged using phase contrast and fluorescence imaging by the IncuCyte® S3 live-cell analysis system (Essen BioScience, USA). Frames were captured at 4-hour intervals in two separate regions per well using a 10X objective. Acquisition times were 350 ms for eGFP and 500 ms for mCherry. Proliferation data were calculated from phase contrast images and fluorescence confluence measurements using the IncuCyte® S3 software. Curves were constructed using Prism 6 (GraphPad Software, USA). Each experiment was performed in triplicate and repeated three times.

2D clonogenic assay

eGFP-OV1946 and mCherry-OV1946 cells were plated at 2 000 cells per well in distinct 6-well plates. The next day, talazoparib diluted in medium was added to the cells at several concentrations from 0 to 4 000 nM and cells were incubated for 7 days. Colonies were stained with methylene blue 0.5% dissolved in methanol (41424, ThermoFisher Scientific) and counted under a stereo microscope. IC_{50} values were calculated using Prism 6 (GraphPad Software). Each experiment was performed at least three times in duplicate.

Acknowledgements

The authors acknowledge Frédérique Labelle for her help with cell culture work. This work was supported by the National Sciences and Engineering Research Council of Canada, the Fonds de recherche du Québec – Nature et technologies, a partnered Cancer Research Society and Ovarian Cancer Canada grant [#20103], and the Canada Foundation for Innovation. Authors acknowledge CMC Microsystems. Access to this expertise is made possible by the TransMedTech Institute and its main funding partner, the Canada First Research Excellence Fund.

References

[1] N. C. Turner and J. S. Reis-Filho, "Genetic heterogeneity and cancer drug resistance," *Lancet Oncol.*, vol. 13, no. 4, pp. e178-85, 2012.

[2] A. Goldman, M. Kohandel, and J. Clairambault, "Integrating Biological and Mathematical Models to Explain and Overcome Drug Resistance in Cancer. Part 1: Biological Facts and Studies in Drug Resistance," *Curr. Stem Cell Reports*, vol. 3, no. 3, pp. 253–259, 2017.

[3] M. Gerlinger and C. Swanton, "How Darwinian models inform therapeutic failure initiated by clonal heterogeneity in cancer medicine," *Br. J. Cancer*, vol. 103, no. 8, pp. 1139–1143, 2010.

[4] Y. Fang and R. M. Eglen, "Three-Dimensional Cell Cultures in Drug Discovery and Development," *SLAS Discov.*, vol. 22, no. 5, pp. 456–472, 2017.

[5] F. Pampaloni, E. G. Reynaud, and E. H. K. Stelzer, "The third dimension bridges the gap between cell culture and live tissue.," *Nat. Rev. Mol. Cell Biol.*, vol. 8, no. 10, pp. 839–45, 2007.

[6] F. Hirschhaeuser, H. Menne, C. Dittfeld, J. West, W. Mueller-Klieser, and L. A. Kunz-Schughart, "Multicellular tumor spheroids: an underestimated tool is catching up again.," *J. Biotechnol.*, vol. 148, no. 1, pp. 3–15, 2010.

[7] A. Frankel, R. Buckman, and R. S. Kerbel, "Abrogation of taxol-induced G2-M arrest and apoptosis in human ovarian cancer cells grown as multicellular tumor spheroids," *Cancer Res.*, vol. 57, no. 12, pp. 2388–2393, 1997.

[8] T. Das *et al.*, "Empirical chemosensitivity testing in a spheroid model of ovarian cancer using a microfluidics-based multiplex platform," *Biomicrofluidics*, vol. 7, no. 1, pp. 011805-1-011805-15, 2013.

[9] A. Fatehullah, S. H. Tan, and N. Barker, "Organoids as an in vitro model of human development and disease," *Nat. Cell Biol.*, vol. 18, no. 3, pp. 246–254, 2016.

[10] M. Astolfi *et al.*, "Micro-dissected tumor tissues on chip: an ex vivo method for drug testing and personalized therapy," *Lab Chip*, vol. 16, pp. 312–325, 2016.

[11] K. Moshksayan *et al.*, "Spheroids-on-a-chip: Recent advances and design considerations in microfluidic platforms for spheroid formation and culture," *Sensors Actuators, B Chem.*, vol. 263, pp. 151–176, 2018.

[12] V. van Duinen, S. J. Trietsch, J. Joore, P. Vulto, and T. Hankemeier, "Microfluidic 3D cell culture: From tools to tissue models," *Curr. Opin. Biotechnol.*, vol. 35, pp. 118–126, 2015.

[13] J. Ruppen *et al.*, “Towards personalized medicine: chemosensitivity assays of patient lung cancer cell spheroids in a perfused microfluidic platform,” *Lab Chip*, vol. 15, no. 14, pp. 3076–3085, 2015.

[14] B. Patra, C.-C. Peng, W.-H. Liao, C.-H. Lee, and Y.-C. Tung, “Drug testing and flow cytometry analysis on a large number of uniform sized tumor spheroids using a microfluidic device,” *Sci. Rep.*, vol. 6, no. 1, p. 21061, 2016.

[15] M. Marimuthu *et al.*, “Multi-size spheroid formation using microfluidic funnels,” *Lab Chip*, vol. 18, pp. 304–314, 2018.

[16] R. Vadivelu, H. Kamble, M. Shiddiky, and N.-T. Nguyen, “Microfluidic Technology for the Generation of Cell Spheroids and Their Applications,” *Micromachines*, vol. 8, no. 4, p. 94, 2017.

[17] P. M. Misun, A. K. Birchler, M. Lang, A. Hierlemann, and O. Frey, “Fabrication and Operation of Microfluidic Hanging-Drop Networks,” in *Cell-Based Microarrays*, 2018, pp. 183–202.

[18] O. Frey, P. M. Misun, D. A. Fluri, J. G. Hengstler, and A. Hierlemann, “Reconfigurable microfluidic hanging drop network for multi-tissue interaction and analysis,” *Nat. Commun.*, vol. 5, p. 4250, 2014.

[19] K. Kwapiszewska, A. Michalczuk, M. Rybka, R. Kwapiszewski, and Z. Brzózka, “A microfluidic-based platform for tumour spheroid culture, monitoring and drug screening.,” *Lab Chip*, vol. 14, pp. 2096–104, 2014.

[20] A. R.Brunet, F. Labelle, P. Wong, and T. Gervais, “Reconfigurable Microfluidic Magnetic Valve Arrays: Towards a Radiotherapy-Compatible Spheroid Culture Platform for the Combinatorial Screening of Cancer Therapies,” *Sensors*, vol. 17, p. 2271, 2017.

[21] C. M. Garvey *et al.*, “A high-content image-based method for quantitatively studying context-dependent cell population dynamics,” *Sci. Rep.*, vol. 6, p. 29752, 2016.

[22] D. R. Caswell and C. Swanton, “The role of tumour heterogeneity and clonal cooperativity in metastasis, immune evasion and clinical outcome,” *BMC Med.*, vol. 15, no. 133, pp. 1–9, 2017.

[23] E. C. Costa, A. F. Moreira, D. de Melo-Diogo, V. M. Gaspar, M. P. Carvalho, and I. J. Correia, “3D tumor spheroids: an overview on the tools and techniques used for their analysis,” *Biotechnol. Adv.*, vol. 34, pp. 1427–1441, 2016.

[24] S. Kessel *et al.*, “High-Throughput 3D Tumor Spheroid Screening Method for Cancer Drug Discovery Using Celigo Image Cytometry,” *SLAS Technol. Transl. Life Sci. Innov.*, vol. 22, no. 4, pp. 454–465, 2016.

[25] M. Zanoni *et al.*, “3D tumor spheroid models for in vitro therapeutic screening: a systematic approach to enhance the biological relevance of data obtained,” *Sci. Rep.*, vol. 6, p. 19103, 2016.

[26] M. Boutros, F. Heigwer, and C. Laufer, “Microscopy-Based High-Content Screening,” *Cell*, vol. 163, no. 6, pp. 1314–1325, 2015.

[27] C. Fang, I. Avis, D. Salomon, and F. Cuttitta, “Novel phenotypic fluorescent three-

dimensional platforms for high-throughput drug screening and personalized chemotherapy," *J. Cancer*, vol. 4, no. 5, pp. 401–415, 2013.

[28] N. Dorst, M. Oberringer, U. Grasser, T. Pohlemann, and W. Metzger, "Analysis of cellular composition of co-culture spheroids," *Ann. Anat.*, vol. 196, no. 5, pp. 303–311, 2014.

[29] D. P. Ivanov *et al.*, "In vitro co-culture model of medulloblastoma and human neural stem cells for drug delivery assessment," *J. Biotechnol.*, vol. 205, pp. 3–13, 2015.

[30] J. C. Waters, "Accuracy and precision in quantitative fluorescence microscopy.," *J. Cell Biol.*, vol. 185, no. 7, pp. 1135–48, 2009.

[31] V. Ljosa and A. E. Carpenter, "Introduction to the Quantitative Analysis of Two-Dimensional Fluorescence Microscopy Images for Cell-Based Screening," *PLoS Comput. Biol.*, vol. 5, no. 12, p. e1000603, 2009.

[32] S.-H. Lu and H. Hua, "Imaging properties of extended depth of field microscopy through single-shot focus scanning," *Opt. Express*, vol. 23, no. 8, p. 10714, 2015.

[33] K. Stock *et al.*, "Capturing tumor complexity in vitro: Comparative analysis of 2D and 3D tumor models for drug discovery," *Sci. Rep.*, vol. 6, p. 28951, 2016.

[34] M. Wartenberg and H. Acker, "Quantitative recording of vitality patterns in living multicellular spheroids by confocal microscopy.," *Micron*, vol. 26, no. 5, pp. 395–404, 1995.

[35] E. A. Susaki *et al.*, "Whole-brain imaging with single-cell resolution using chemical cocktails and computational analysis," *Cell*, vol. 157, no. 3, pp. 726–739, 2014.

[36] S. M. Grist, S. S. Nasseri, T. Poon, C. Roskelley, and K. C. Cheung, "On-chip clearing of arrays of 3-D cell cultures and micro-tissues," *Biomicrofluidics*, vol. 10, no. 4, pp. 1–15, 2016.

[37] M. Makale *et al.*, "Extended-working-distance multiphoton micromanipulation microscope for deep-penetration imaging in live mice and tissue," *J. Biomed. Opt.*, vol. 14, no. 2, p. 024032, 2009.

[38] S. P. Cavnar, E. Salomonsson, K. E. Luker, G. D. Luker, and S. Takayama, "Transfer, Imaging, and Analysis Plate for Facile Handling of 384 Hanging Drop 3D Tissue Spheroids," *J. Lab. Autom.*, vol. 19, no. 2, pp. 208–14, 2014.

[39] S. Kummar *et al.*, "Advances in using PARP inhibitors to treat cancer," *BMC Med.*, vol. 10, no. 1, p. 25, 2012.

[40] V. Malhotra and M. C. Perry, "Classical Chemotherapy: Mechanisms, Toxicities and the Therapeutc Window," *Cancer Biol. Ther.*, vol. 2, pp. S2–S4, 2003.

[41] V. Ouellet *et al.*, "Characterization of three new serous epithelial ovarian cancer cell lines.," *BMC Cancer*, vol. 8, p. 152, 2008.

[42] A. St-Georges-Robillard *et al.*, "Fluorescence hyperspectral imaging for live monitoring of multiple spheroids in microfluidic chips," *Analyst*, vol. 143, no. 16, pp. 3829–3840, 2018.

[43] P. Tofilon, N. Buckley, and D. Deen, "Effect of cell-cell interactions on drug sensitivity and growth of drug-sensitive and -resistant tumor cells in spheroids," *Science*, vol. 226, no. 4676, pp. 862–864, 1984.

[44] N. Rousset, F. Monet, and T. Gervais, “Simulation-assisted design of microfluidic sample traps for optimal trapping and culture of non-adherent single cells, tissues, and spheroids,” *Sci. Rep.*, vol. 7, p. 245, 2017.

[45] B. Patra *et al.*, “Are 3D spheroids always more resistant to chemotherapy than 2D cultures? A chip-based survey using ovarian cancer cell lines,” in *Proceedings of MicroTAS 2016*, 2016, pp. 1555–1556.

[46] J. Friedrich, R. Ebner, and L. A. Kunz-Schughart, “Experimental anti-tumor therapy in 3-D: Spheroids – old hat or new challenge?,” *Int. J. Radiat. Biol.*, vol. 83, no. 11–12, pp. 849–871, 2007.

[47] I. C. McLean, L. A. Schwerdtfeger, S. A. Tobet, and C. S. Henry, “Powering ex vivo tissue models in microfluidic systems,” *Lab Chip*, vol. 18, no. 10, pp. 1399–1410, 2018.

Figures

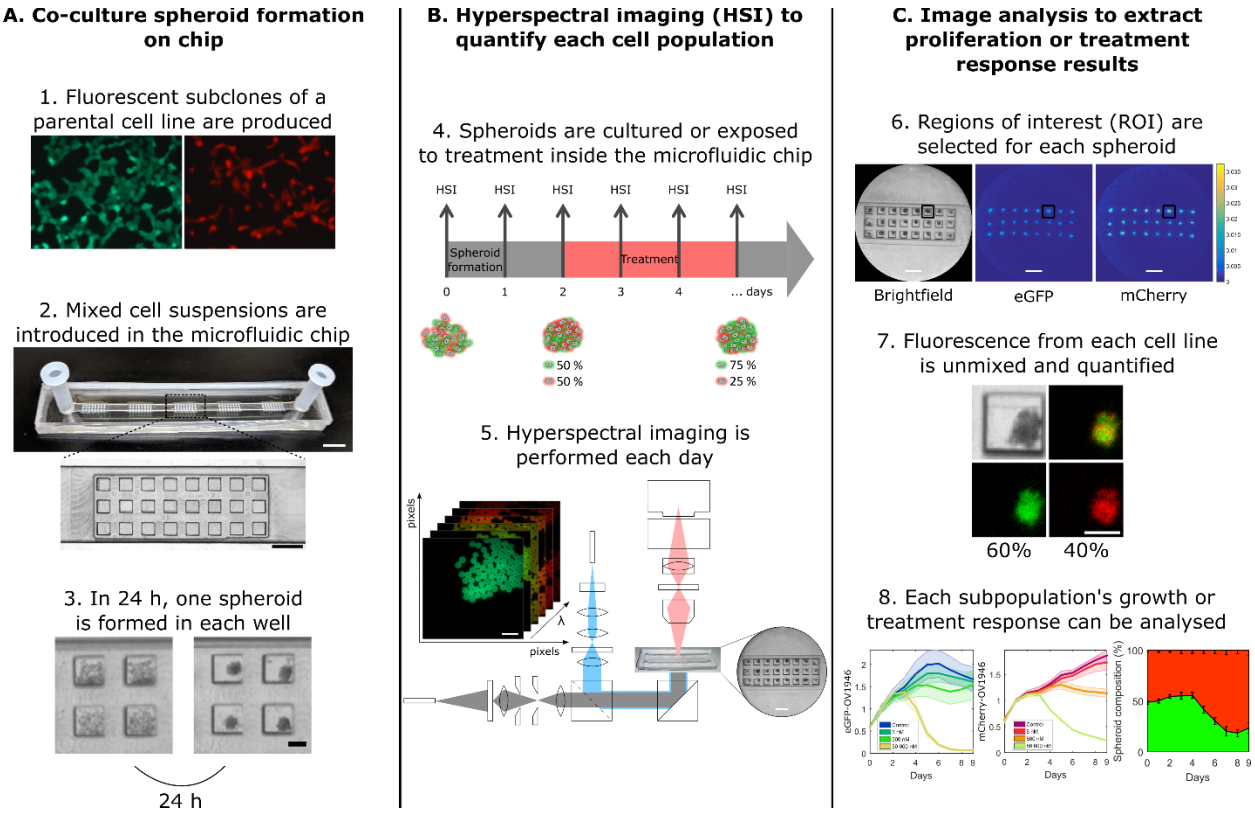

Figure 1. Co-culture spheroid assay using hyperspectral imaging workflow. A) Fluorescent subclones of the same parental cell line were first generated by transfecting OV1946 cells. For one subclone, all cells express the fluorescent protein (eGFP or mCherry) at similar levels due to a limited dilution selection. Co-culture spheroids are then formed on-chip by introducing a cell suspension containing both subclones in the main channel of the microfluidic chip. Cells sediment into the wells and form spheroids in 24 h. Scale bars in 2 represent 6 and 1 mm and scale bar in 3 represents 250 µm. B) Spheroids are cultured in the microfluidic chip and medium, in which drugs can be added, is changed daily. A custom-built HSI system [42] was then used to image and quantify the spheroids' fluorescence at multiple time-points. C) HSI images were processed to remove any system response. Regions of interest (ROI) corresponding to each well of the microfluidic chip were determined and spectral unmixing was performed to separate the spectral entities. Fluorescence intensities from each fluorescent protein were normalised to the reference intensity and the spheroid composition, a percentage of each subclone, was calculated. Using the fluorescent protein intensity and the spheroid compositions over time, the co-culture spheroid response to external stimuli could be analysed. Scale bar in 7 represents 250 µm and other scale bars not specified represent 1 mm.

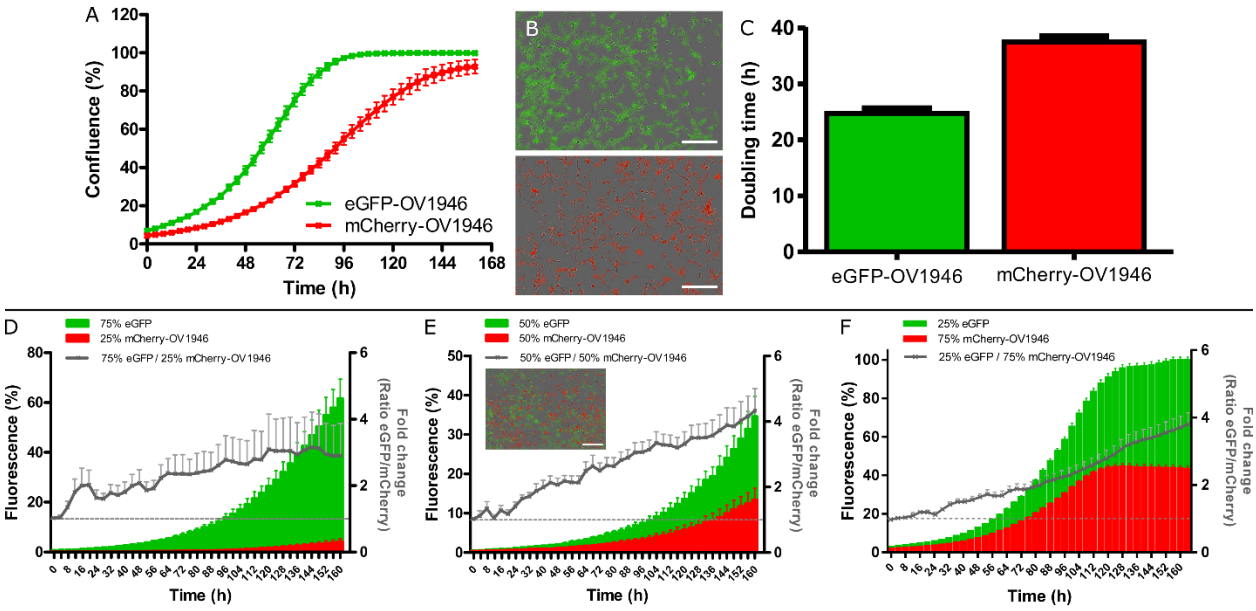

Figure 2. 2D cell population proliferation in monolayer culture. A) Representative example of the cell growth over time. B) Fluorescence images at 96 h, and C) average doubling time (n = 3) of each subclone cultured separately. D-F) Representative example (n = 1) of the proliferation over time of each subclone cultured together at various ratios: 75:25 (D), 50:50 (E, inset shows a fluorescence image at 96 h), and 25:75 (F). Grey curves show the fold change (normalised to 1) of the ratio between eGFP and mCherry fluorescence. Scale bars = 300 µm.

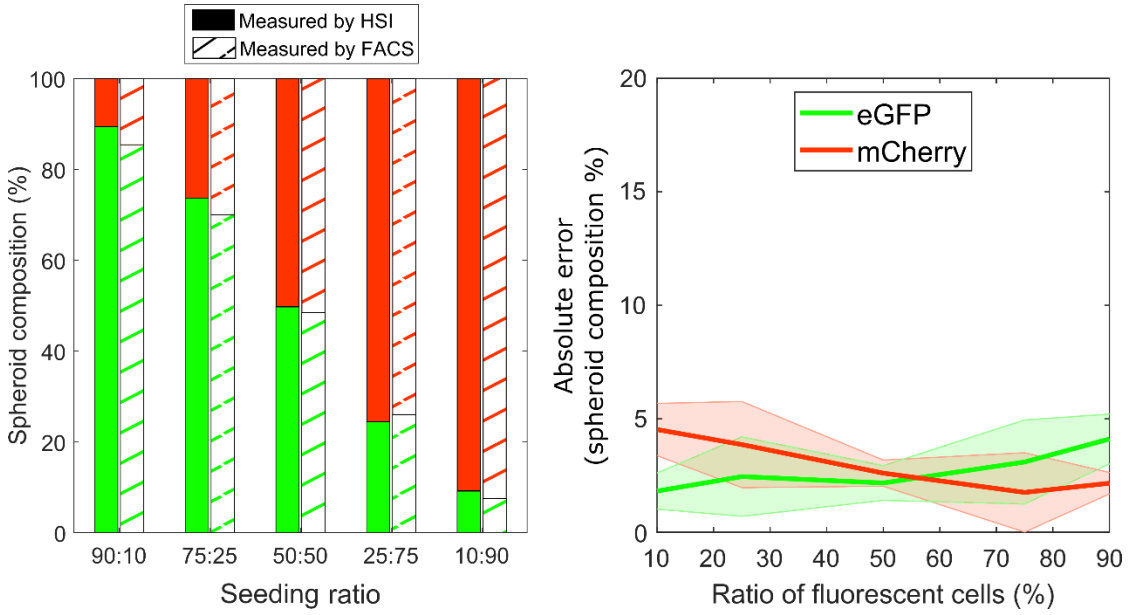

Figure 3. FACS validation of HSI measurements. A) Comparison of spheroid composition measurements obtained by HSI and by FACS (representative example of n = 1). B) Absolute error of HSI measurements compared to FACS. Shaded regions indicate the standard deviation of the calculated error (n = 3).

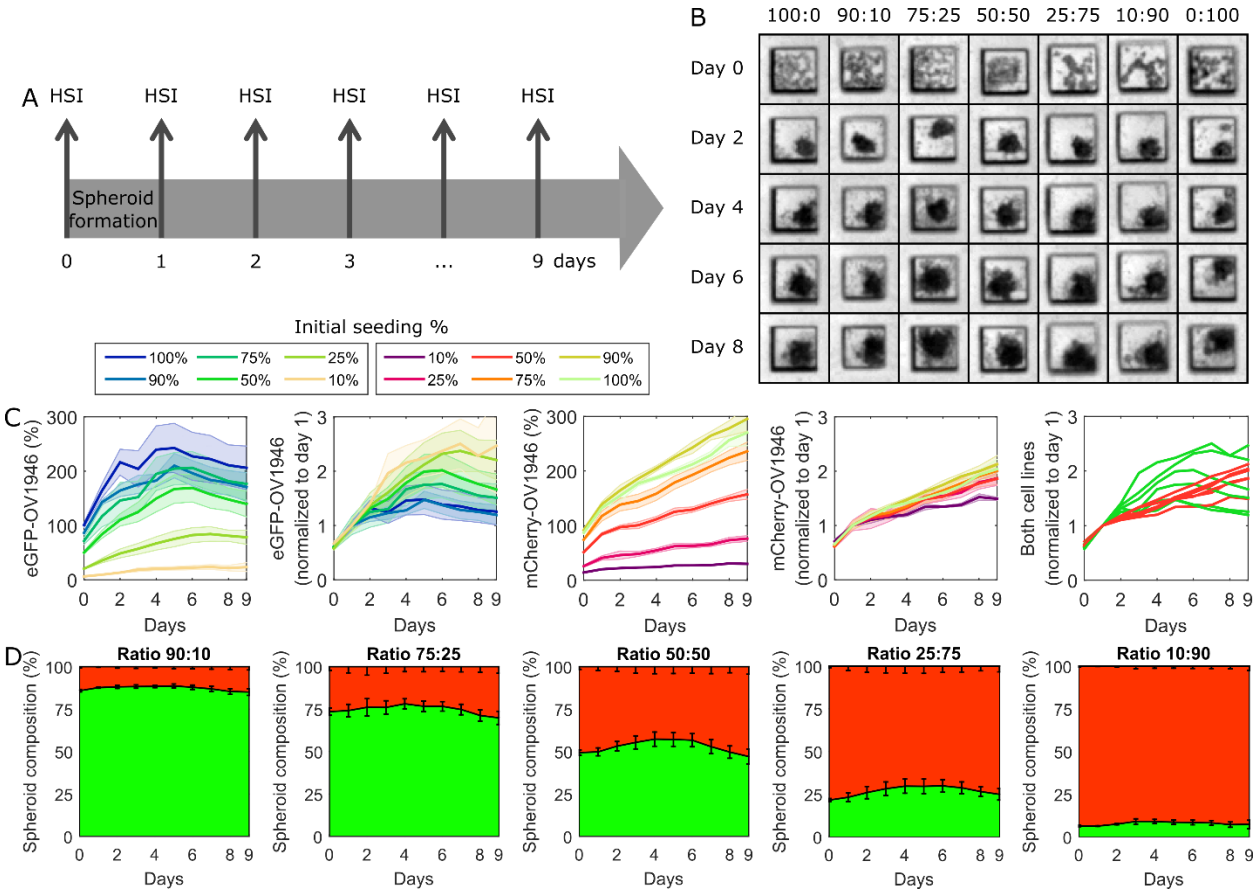

Figure 4. Cell population proliferation in co-culture spheroids. A) Experiment timeline. B) Brightfield images of spheroids over time. For a specific seeding ratio, the same spheroid is shown over time. C i-ii) eGFP-OV1946 and C iii-iv) mCherry-OV1946 proliferation according to the initial cell seeding ratio. In C ii and iv, curves from i and iii are normalised to day 1. C v) Comparison of the proliferation rates normalised to day 1 of both fluorescent clones (same data as in C ii and iv). D i-v) Evolution over time of spheroid composition according to initial seeding ratio (bottom/green: eGFP; top/red: mCherry). Shaded regions or error bars represent the standard error of the mean (n = 3).

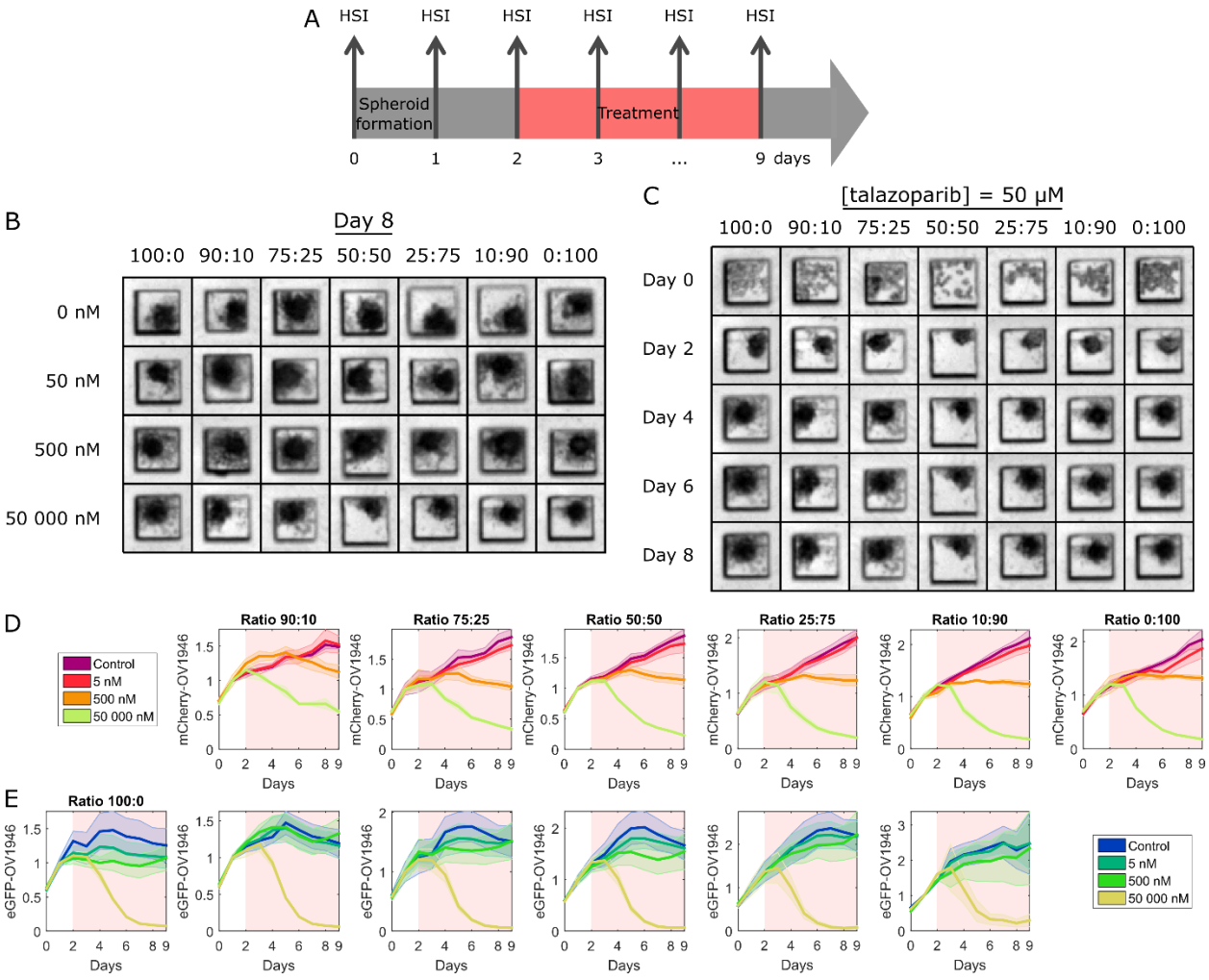

Figure 5. Treatment response assay using talazoparib. A) Experiment timeline. B) Brightfield images of spheroids at day 8, relevant to the drug concentration. C) Brightfield images of spheroids over time, for a talazoparib concentration of 50 µM. For a specific seeding ratio, the same spheroid is shown over time to observe its response to the drug. D i-vi) Day 1-normalised mCherry-OV1946 response to different concentrations of talazoparib, according to the initial seeding ratio. E i-vi) Day 1-normalised eGFP-OV1946 response to different concentrations of talazoparib, according to the initial seeding ratio. Shaded regions represent the standard error of the mean (n = 3).

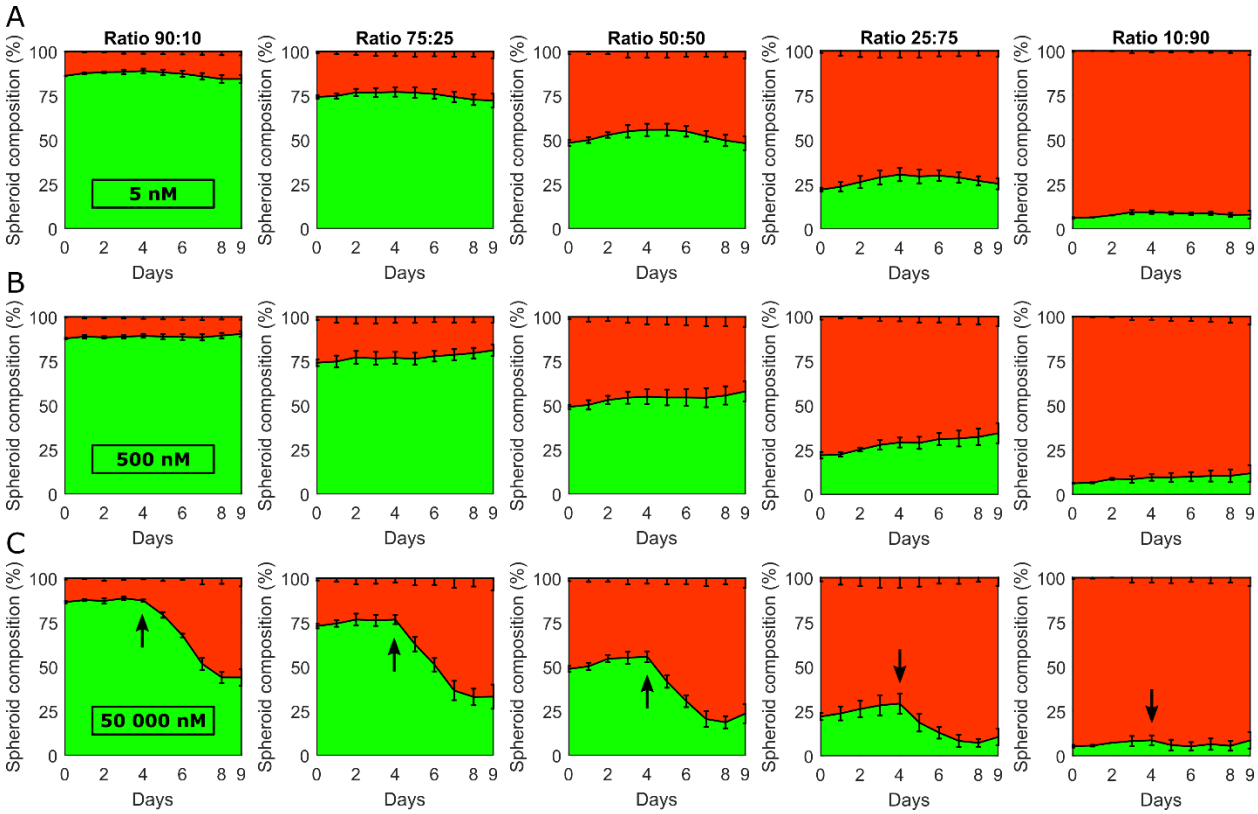

Figure 6. Spheroid composition as a response to talazoparib applied from day 2 to day 9. Spheroid composition over time, according to the initial seeding ratio for a talazoparib concentration of A) 5 nM, B) 500 nM, and C) 50 µM. Control data (for a talazoparib concentration of 0 nM) is shown in Fig. 4D. For all graphs, bottom/green represent eGFP and top/red, mCherry. Arrows indicate clonal takeover onset. Error bars represent the standard error of the mean (n = 3).

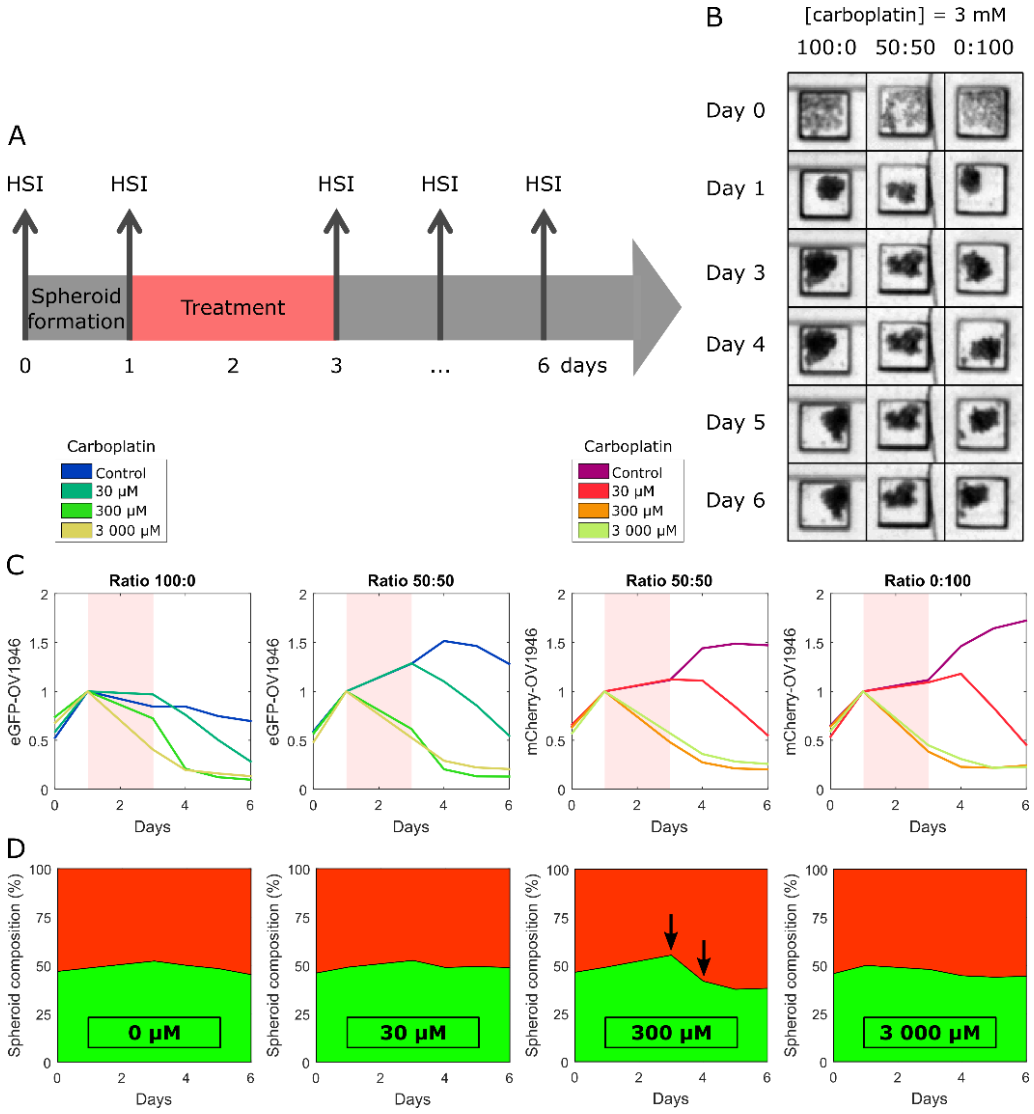

Figure 7. Treatment response assay using carboplatin. A) Experiment timeline. B) Brightfield images of spheroids over time, for a carboplatin concentration of 3 mM. For a specific seeding ratio, the same spheroid is shown over time to observe its response to the drug. Brightfield images could not be acquired for 100:0-day 6 and 50:50-day 3. C i-ii) Day 1-normalised eGFP-OV1946 response to different concentrations of carboplatin, according to the initial seeding ratio. C iii-iv) Day 1-normalised mCherry-OV1946 response to different concentrations of carboplatin, according to the initial seeding ratio. D) Spheroid composition over time (bottom/green: eGFP; top/red: mCherry). Each curve represents the average of 24 spheroids (n = 1). Arrows indicate differences in behaviour of the two subclones.

Supplementary material

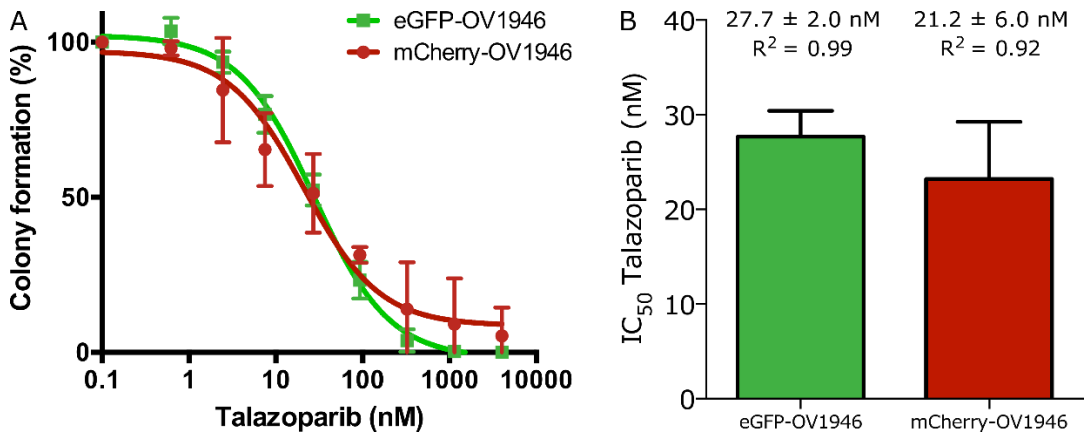

Figure S1. Determination of the 2D IC_{50} by clonogenic assay for both subclones. A) Average dose-response curves for both subclones. B) Talazoparib IC_{50} for eGFP-OV1946 and mCherry-OV1946, p = 0.655. Error bars represent the standard deviation (n = 3).

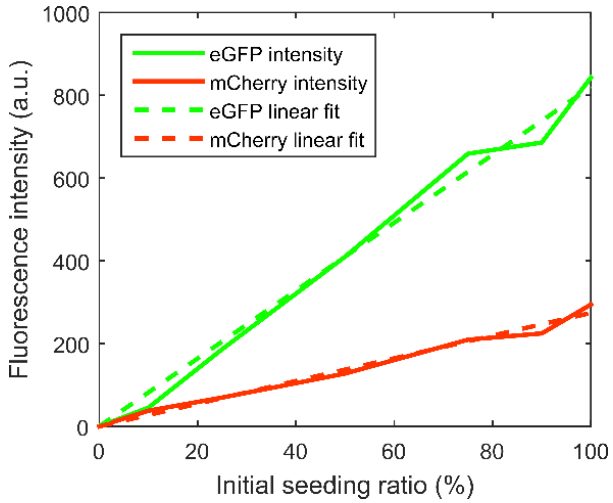

Figure S2. Reference intensity linear fitting for eGFP and mCherry fluorescence comparison.